Supramolecular Photosystem II Organization in Grana Thylakoid Membranes: Evidence for a Structured Arrangement†

Helmut Kirchhoff,*,‡ Ira Tremmel,‡,⊥ Winfried Haase,|| and Ulrich Kubitscheck§

Institut für Botanik, Schlossgarten 3, D-48149 Münster, Germany, Environmental Biology Group, Research School of Biological Sciences, Australian National University, Canberra, A.C.T. 2601, Australia, Max-Planck-Institut für Biophysik, Marie-Curie-Strasse 15, D-60439 Frankfurt am Main, Germany, and Institut für Medizinische Physik und Biophysik, Robert-Koch-Strasse 31, D-48149 Münster, Germany

Received March 18, 2004; Revised Manuscript Received April 29, 2004

ABSTRACT: The distribution of photosystem (PS) II complexes in stacked grana thylakoids derived from electron microscopic images of freeze-fractured chloroplasts are examined for the first time using mathematical methods. These characterize the particle distribution in terms of a nearest neighbor distribution function and a pair correlation function. The data were compared with purely random distributions calculated by a Monte Carlo simulation. The analysis reveals that the PSII distribution in grana thylakoids does not correspond to a random protein mixture but that ordering forces lead to a structured arrangement on a supramolecular level. Neighboring photosystems are significantly more separated than would be the case in a purely random distribution. These results are explained by structural models, in which boundary lipids and light-harvesting complex (LHC) II trimers are arranged between neighboring PSII. Furthermore, the diffusion of PSII was analyzed by a Monte Carlo simulation with a protein density of 80% area occupation (determined for grana membranes). The mobility of the photosystems is severely reduced by the high protein density. From an estimate of the mean migration time of PSII from grana thylakoids to stroma lamellae, it becomes evident that this diffusion contributes significantly to the velocity of the repair cycle of photoinhibited PSII.

In higher plants, the conversion of light energy into metabolically usable forms by photosynthesis takes place at the thylakoid membrane in the chloroplasts. The mature membrane is folded into a complex three-dimensional network in which two structural elements can be distinguished (*1*, *2*). About 80% of the membrane consists of strictly stacked membrane disks (grana thylakoids) with a cylindrical shape and a diameter of about 0.5 μm. These membrane disks are interconnected by unstacked stroma lamellae. The protein complexes involved in energy transduction are inhomogeneously distributed between these subcompartments (*3*). Photosystem (PS)[1] II and light-harvesting complex (LHC) II are concentrated in the stacked grana areas, whereas PSI, LHCI, and ATPase complexes are found in the unstacked areas. The distribution of the cytochrome (cyt) bf complex is still under discussion but is assumed to be homogeneous. Energy transduction in this system comprises a sequence of electron-transfer reactions by which water is oxidized and $NADP^+$ reduced. Water splitting takes place at PSII. The electrons liberated by this process are transferred to plastoquinone in a reaction mediated by PSII. Plastoquinone is the only electron-transfer component that is not protein-bound. It diffuses in the hydrophobic membrane phase and passes electrons onto the cyt bf complex. From here, electrons are transferred to plastocyanin, which diffuses in the thylakoid lumen to PSI, which in turn passes these, via ferredoxin, to $NADP^+$. The energy for the strongly endergonic electron-transfer reactions occurring in the reactions centers of the two photosystems comes in the form of excitons. Each reaction center is functionally coupled to several hundreds of accessory pigments (mainly chlorophylls) bound to light-harvesting complexes. The light-harvesting complexes have the important function of efficiently passing absorbed light energy to the reaction centers.

In the past decade, significant progress has been made in elucidating the structure of the protein complexes involved in photosynthetic energy transduction (*4*−*8*). Furthermore, evidence has emerged that the protein complexes in the native thylakoid membrane form relatively stable, more highly organized supercomplexes. Supercomplexes have been described for the LHCII ($LHCII_3$), (*9*, *10*), the cyt bf complex, $(cyt\ bf)_2$ (*11*, *12*), PSI with LHCI, PSI−$(LHCI)_4$, (*13*) and PSII with LHCII, $(PSII-LHCII_3)_2$, (*14*, *15*). The PSII supercomplex has been investigated intensively. It is located in the grana area, and the antenna of each PSII monomer within the dimer consists of the core antenna proteins CP43 and CP47, as well as the minor antenna proteins Lhcb4 (CP29), Lhcb5 (CP26) and Lhcb6 (CP24) and a strongly

† H. K. is supported by the Deutsche Forschungsgemeinschaft (Grant KI 818/2-1).

* Corresponding author. Phone: +49 251 8324820. Fax: +49 251 8323823. E-mail: kirchhh@uni-muenster.de.

‡ Institut für Botanik.

⊥ Australian National University.

|| Max-Planck-Institut für Biophysik.

§ Institut für Medizinische Physik und Biophysik.

[1] Abbreviations: cyt, cytochrome; chl, chlorophyll; LHC, light-harvesting complex; NNDF, nearest neighbor distribution function; PCF, pair correlation function; PQ, plastoquinone; PS, photosystem.

10.1021/bi0494626 CCC: $27.50
Published on Web 06/24/2004

bound LHCII trimer (probably composed of two Lhcb1 and one Lhcb2) (*16*). The supercomplex is furthermore associated with loosely bound LHCII trimers in a way that 230−250 chlorophyll molecules are interacting with each reaction center (*10*). Therefore, two LHCII pools exist: an inner (strongly bound) pool, which is part of the $(PSII-LHCII_3)_2$, and a "peripheral" (more loosely bound) pool (*17*). An alternative model for PSII organization has PSII as a monomer in the grana area (*18*); however, in addition to structural evidence (see *19* for a review), there are also arguments from biochemical and functional research suggesting that PSII in the grana core is organized as a $(PSII-LHCII_3)_2$ (*20, 21*). The $(PSII-LHCII_3)_2$ supercomplex has been isolated from spinach (*22*), Chlamydomonas (*23*), Arabidopsis (*24*), and the liverwort Marchantia (*25*) and has been structurally characterized with a resolution of about 2.4 nm. The structures were found to be almost identical. This can be taken as an indication that supercomplexes are a widespread phenomenon in higher plants.

In contrast to the supermolecular level, little is known about the structural cooperation of protein complexes at the higher, supramolecular, level. In particular, the relationship between the peripheral LHCII pool and the PSII supercomplex has not yet been clarified. Recently, associations of one or more LHCII trimers with the $(PSII-LHCII_3)_2$ supercomplex in the grana area have been described (*25, 26*). This became possible through careful isolation procedures and a sophisticated analysis of electron microscopic images. An important finding of these studies is that the peripheral LHCIIs do not bind arbitrarily on the PSII supercomplex; rather, there are specific binding sites. Whether these associations also exist in the native membrane and how multiple supercomplexes might be arranged together is still unknown. The arrangement of protein complexes in grana thylakoids is potentially highly flexible. This was impressively visualized by early electron microscopic images of freeze-fractured thylakoid membranes (e.g., see ref *27*). Such studies show that incubation of membranes in low-salt media leads to a rearrangement of protein complexes from a seemingly random distribution to a highly ordered paracrystalline arrangement. In further studies, such two-dimensional (2D) crystalline protein arrangements have frequently been described in grana thylakoids but never in stroma lamellae (*28*−*32*). It has been found that the 2D crystals can consist of PSII supercomplexes as well as LHCII trimers. 2D arrays play an important role in the molecular and supermolecular structural elucidation of PSII and LHCII. In the native membrane, however, the protein complexes appear to be randomly distributed (*24, 27, 29*, see also the review in ref *19*). It is still an open question whether paracrystalline protein arrangements exist in native grana thylakoids alongside the random organization. Crystalline arrangements appear more often if the membranes are treated with detergents (*28, 31*), if they are destacked in media with low ionic strength (*27*), or in cold-stressed plants (*29, 31*). The latter has not yet been systematically examined but opens up the interesting possibility that the saturation level of fatty acids could have an important influence on supramolecular protein organization, as discussed in ref *31*.

One question that remains open is whether the seemingly random protein arrangement in grana membranes is indeed purely random or if there is a certain degree of order. Here, the terms random, on one hand, and ordered or structured, on the other hand, will be used to distinguish the absence or presence of interactions between the particles. The human eye is not a reliable instrument to evaluate the randomness of a distribution. Instead, we have used an approach based on objective mathematical methods to analyze the protein distribution in the grana core of isolated chloroplasts.

The supramolecular organization of protein complexes in grana thylakoids is of great physiological relevance for the photosynthetic energy transduction. For example, there are indications that the PQ diffusion in a random protein arrangement is not efficient (*33*−*35*). It was suggested that inefficient PQ diffusion could be prevented through a structured arrangement of PSII and LHCII complexes. It is possible that an altered protein arrangement could disturb PQ diffusion, which would in turn have a direct influence on its redox state. The redox state of the PQ pool in turn functions as a central sensor in the thylakoid membrane, regulating adaptations of the photosynthetic apparatus. Processes shown to be governed by the PQ redox status are the reversible phosphorylation of LHCII and PSII subunits (*36*−*38*) and, more recently, differential control of photosynthetic gene expression (*39*). Furthermore, sustained overreduction of the PQ pool leads to irreversible photoinhibition of PSII (*37, 40*). In this process, the D1 subunit of PSII is damaged, due to the formation of triplet oxygen. Damaged PSII must diffuse from the grana into the stroma lamellae, where the damaged D1 is replaced by a de-novo synthesized polypeptide. The reassembled PSII then migrates back to the grana area. The supramolecular protein arrangement in the granum could play an important role in this lateral trafficking. Additionally, the spatial organization of protein complexes in the granum could influence the flow of energy in the PSII antenna system. It is well established that, in the grana area, multiple PSII reaction centers exist in excitonic contact, mediated by LHCII (*41*). It has long been known that in artificially destacked thylakoids with a randomized protein arrangement cooperativity between the PSII complexes is lost (*42* and references therein). In such a randomly organized membrane, exciton transfer in the antenna system of PSII is obviously disturbed. These examples illustrate how closely the function and regulation of energy transduction are coupled to the supramolecular organization of protein complexes in grana thylakoids.

We have used statistical methods to characterize particle distributions in terms of the nearest neighbor distribution function (NNDF) and the pair correlation function (PCF) to determine whether PSII distribution in grana membranes is random (*43*−*45*). This analysis also allows the comparison of different distributions. The exact positions of PSII in the membranes were obtained from electron microscopic pictures of freeze-fractured thylakoid membranes from isolated chloroplast. Freeze fracture splits the thylakoid membrane at its hydrophobic center, thus producing two half-membranes, the so-called protoplasmatic (PF) and exoplasmatic half-membrane (EF). The half-membranes originating from the stacked thylakoid area are labeled with the subscript s (EF_s, PF_s) and those originating from the unstacked area are labeled with the subscript u (EF_u, PF_u) (*2*). From a series of studies, it has been clearly established that PSII is exclusively found in the EF half-membrane (for review, see ref *2*). NNDF and PCF data derived from these electron microscopic pictures

were compared with purely random distributions of the grana protein complexes generated by Monte Carlo methods. This comparison suggests the existence of order in grana thylakoids.

MATERIAL AND METHODS

Chloroplast and Grana Membrane Preparation. Chloroplasts were isolated from 6-week-old leaves of spinach (*Spinacea oleraceae* var. polka) grown in a hydroponics medium (*46*) at 13−16 °C according to procedures in ref *33*. The photoperiod was 10 h (300 μmol quanta m^{-2} s^{-1}). Grana thylakoids were isolated from the chloroplasts according to procedures in ref *47* (BBY membranes) with slight modifications. In detail, chloroplasts were centrifuged (2500 × *g*, 5 min), and the pellet was resuspended in 150 mM NaCl, 5 mM $MgCl_2$, and 20 mM Tricine, pH 8.0 (NaOH), and centrifuged again. The thylakoids in the pellet were resuspended in 15 mM NaCl, 5 mM $MgCl_2$, 0.4 M sucrose, and 20 mM 2-(morpholino)-ethanesulfonic acid (MES), pH 6.5 (NaOH) (buffer C). The chlorophyll content was determined according to the procedure in ref *48*. The thylakoid suspension was diluted to 5 mg/mL chlorophyll. Triton X-100 (Sigma Aldrich) in buffer C was slowly added on ice to a final concentration of 5% (w/w). After 15 min incubation, the solution was centrifuged (28 000 × *g*, 30 min), and the pellet was resuspended in detergent-free buffer C and centrifuged again (2000 × *g*, 5 min) to remove starch. After centrifugation of the supernatant (28 000 × *g*, 30 min), the grana membranes were resuspended in buffer C, and the chlorophyll concentration was determined.

Quantification of LHCII, PSII, and cyt bf Complex. The LHCII (Lhcb1−3) content of BBY membranes was determined by quantitative SDS−PAGE gel analysis, comparing the Coomassie staining of BBY membranes with isolated LHCII (*34*). A chlorophyll-to-protein ratio of 14 was assumed for the calculation of moles of isolated LHCII proteins from the chlorophyll content (*4*, *10*).

The PSII content was derived from the light pulse induced difference absorption signal of pheophytin at 550 minus 540 nm as described in detail in ref *34*. The chlorophyll content was 50 μM. Typically 10 measurements per wavelength were averaged. It was confirmed that this quantification is not dependent on the intactness of the water splitting system. This can be concluded from comparing measurements with an intact water splitting system with water splitting inactivated by a hydroxylamine treatment.

The cytochrome bf complex was quantified from chemically induced absorbance changes of cytochrome f and cytochrome b6 as described in ref *34*. The validity of the quantification is supported by the result that the stoichiometry of cytochrome b6 to cytochrome f is 1.9 ± 0.1 ($n = 3$).

Freeze-Fracture Electron Microscopy. Isolated membranes in suspension were loaded onto specimen holders (small copper plates) and frozen in ethane cooled by liquid nitrogen. Freeze fracturing was performed in a BAF400T freeze-fracture apparatus (Balzers, Lichtenstein) keeping the specimen stage at −150 °C. Platinum/carbon shadowing was carried out with an electron gun kept at an angle of 45° between evaporation source and specimen stage. Carbon-reinforced (carbon evaporation at 90°) replicas were cleaned in chromo-sulfuric acid, washed in water, and collected on Formvar film-coated copper grids for analysis in an electron microscope (EM208S, Philips, Eindhoven, The Netherlands). Images were taken at a magnification of 13 000 with a CCD camera (TVIPS 1K × 1K slow-scan CCD camera).

Monte Carlo Calculations. The Monte Carlo calculations were carried out for a square lattice. Periodic boundary conditions were assumed, that is, the actual shape of the lattice corresponded to a torus. Consequently, a particle that was positioned at one edge of the lattice was continued at the opposite side. The lattice spacing was chosen as 1 nm. This is related to the typical size of lipids.

For the diffusion analysis of PSII, initially randomly distributed obstacles were placed on the lattice at the required concentrations as described in ref *35*. Then, at each step, the proteins were allowed to move to an immediately adjacent unoccupied site by a random walk (diagonal movements were not considered). For nonspherical particles, for example, particles with the shape of photosynthetic proteins, the exact calculation of their translation and rotation in a membrane is very difficult due to the viscosity of the membrane. Therefore some simplifications were needed. Accordingly, it was assumed that translation in all dimensions was equally probable. Furthermore, it was assumed that at each step each particle rotated about ±10°. That is, forces tangential to the body surface (viscosity of the matrix molecules) and forces normal to the surface (pressure forces caused by momentum transfer between the particles and the matrix molecules) were not addressed directly but subsumed into the ratio of rotational energy to translational energy. This is somewhat arbitrary but the exact degree of rotation should not influence the general outcome. The pseudo-random number generator used (*49*) produces more than 2×10^{18} random numbers (see also ref *50*). All particles were moved with the same probability, regardless of their size.

NNDF and PCF Analysis of Particle Distributions. The Cartesian coordinates representing the position of PSII in the imaged portion of a freeze-fracture membrane area were determined experimentally. These were used to calculate the distances between individual PSIIs. Estimators for the nearest neighbor distribution function (NNDF) and the pair correlation function (PCF) were used according to procedures in refs *51* and *52*. Standard techniques (*52*, *53*) were also used to deal with the edge effects of the finite sample spaces. For comparison, the distribution functions were also calculated for truly random distributions, calculated by Monte Carlo simulations.

(a) Nearest Neighbor Distribution Function. This function, $d(r)$, is determined by measuring the nearest-neighbor distance for each particle of the sample. Then, the accumulated frequency of the nearest neighbor distances is plotted versus distance. Specifically,

$$d(r) = P(\text{distance from a typical particle to the nearest particle of the sample is at most } r)$$

where P designates the accumulated probability.

Figures 2A and 4A do not show the NNDF directly but the distribution of nearest neighbor distances.

(b) Pair Correlation Function. The distance distribution of objects is determined by their pair correlation function, PCF(r) (*54*). When a typical central object is chosen, the

Table 1: Characterization of the Chloroplast and BBY Membrane Preparation

	chloroplasts	grana preparation
PSII	2.60 (SD[b] 0.10) mmol/mol chl	3.97 (SD[b] 0.25) mmol/mol chl
LHCII[a]	*c*	47.62 (SD[b] 2.08) mmol/mol chl
cyt bf complex	1.31 (SD[b] 0.08)	*c*
chl a/b	3.10 (SD[b] 0.05)	2.28 (SD[b] 0.01)

[a] Lhcb1−3 gene products. The numbers are the mean value of at least three determinations. [b] Standard deviation. [c] Not detected.

average number of objects $n(r)dr$ located in a shell of radii r and $r + dr$ is given by

$$n(r)dr = \rho \mathrm{PCF}(r) 2\pi r dr$$

Therefore, the PCF(r) quantifies deviations of the local density from the average density in a ring r, $r + dr$ around a typical object. For randomly distributed point objects, $\mathrm{PCF}_{\mathrm{random}}(r) = 1$ for $r > 0$, because there exist, on average, no deviations between local and global density (ρ).

RESULTS

Characterization of the Membrane Preparations. The compositions of thylakoid membranes of isolated chloroplasts and BBY membranes are summarized in Table 1. The Monte Carlo simulation performed in this study requires knowledge of the ratio of LHCII trimers to PSII in the membranes. For stacked grana membranes, we calculated a ratio of 4.0 ± 0.4 (47.62 LHCII monomers/(3 × 3.97 PSII)) from Table 1. This corresponds well with values in the literature (*55*).

From electron microscopic images of freeze-fractured chloroplasts, an EF_s face particle density of 1701 ± 49 μm^{-2} can be deduced (12 EF_s pictures were analyzed). This value is in the density range reported for the grana region of intact thylakoids, which is between 1500 and 2000 μm^{-2} (*2*). The EF_s particles represent exclusively PSII complexes (*2*). Assuming that PSII in the stacked grana region is organized as the $(PSII-LHCII_3)_2$ supercomplex (see the introduction section), the EF_s particle density directly represents the PSII supercomplex density. From the ratio of LHCII trimers to PSII of 4.0 ± 0.4, the density of the peripheral LHCII trimer pool (not firmly bound in the $(PSII-LHCII_3)_2$ supercomplex) can be estimated to be 10 206 ± 1315 μm^{-2} (1701 × 2 × 4 − 1701 × 2). In principle, the LHCII trimer density can also be deduced from the electron microscopic images of the PF half-membrane. However, because of the significantly higher density and the smaller diameter of LHCII, it is difficult to detect these particles in electron microscopic images of freeze-fractured membranes in a reliable way.

Analysis of the EF_s Distribution in Chloroplasts. To determine the PSII distribution in stacked grana areas, EM pictures of the EF_s region of freeze-fractured chloroplasts were analyzed. The EF_s regions are easy to identify: on one hand, they differ clearly from the PF regions in having bigger particles; on the other hand, there is a lower particle density in EF_u compared to the EF_s half-membrane (*2*).

Figure 1A shows a typical part of an EM picture of the EF_s half-membrane. The coordinates of the EF_s particles (Figure 1B) were determined as the centers of the outlined objects. The analysis of the particle distribution derived from

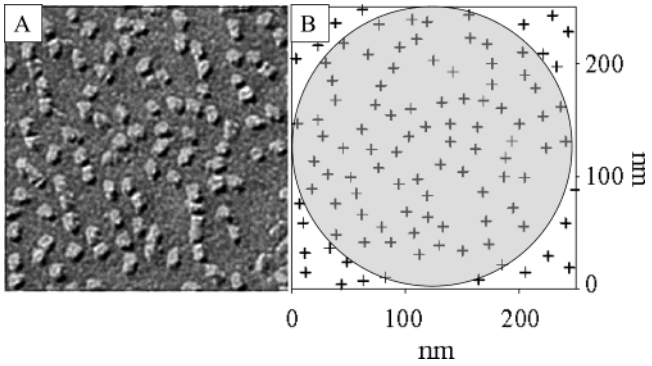

FIGURE 1: Determination of photosystem II positions in grana membranes. Panel A shows an example of a 250 nm × 250 nm sized electron micrograph from the EF_s face of freeze-fractured chloroplasts. Each particle represents a PSII complex. Magnification is 356 000×. In panel B, the exact position of each PSII was determined from the lined EF_s particle with the program Optimas 6.5. The program calculates the center of each particle (crosses) from the lined area.

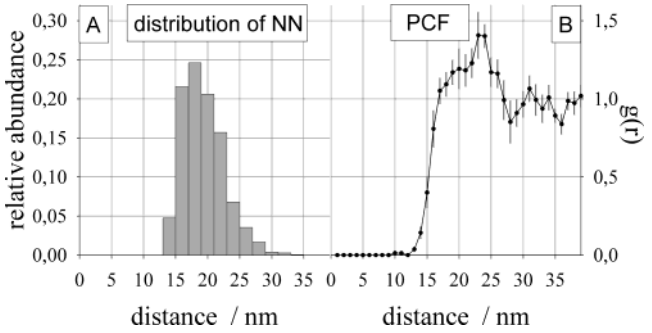

FIGURE 2: Analysis of PSII distribution in grana membranes. Panel A shows the distribution of next neighbor distances. For the distribution of next neighbor distances, particle positions shown in the gray-colored area in Figure 1B were analyzed. A total of 1016 particles from 12 micrographs were analyzed and averaged. Panel B shows the PCF analysis. The PCFs were determined from the same set of particle positions. Looking from a given PSII, the PCF gives the deviation of the local PSII density from the mean density as a function of distance. Error bars indicate the standard error of the mean.

the EF_s coordinates is shown in Figure 2. From the distribution of next neighbor distances (Figure 2A), it follows that for more than 80% of the EF_s particles the distance to the next photosystem is between 15 and 23 nm. We assume that, in the stacked region of the granum, PSII is organized as $(PSII-LHCII_3)_2$ supercomplexes (see the introduction section). This complex has an almost rectangular contour with a dimension of 12 nm × 27 nm (*14*, *15*, *19*). In a first approximation, the distance between two neighboring PSII supercomplexes in the granum corresponds to their own size. This explains the high density of PSII in grana thylakoids (see also Figure 3A for a visualization). From the EF_s particle density of 1701 μm^{-2} and the molecular area of the $(PSII-LHCII_3)_2$ supercomplexes of 285 nm^2 (*34*), it follows that PSII supercomplexes occupy 48% of the total area. The relative area occupation of peripheral LHCII and cyt bf complexes (assuming a cyt bf to PSII ratio of 0.5, see below) calculated in the same way is around 38% (10206 $(LHCII)_3$ μm^{-2} × 34 nm^2 + 851 $(cyt\ bf)_2$ μm^{-2} × 51 nm^2). Therefore, more than 80% of the total area in a grana thylakoid membrane is covered by protein complexes.

The PCF (Figure 2B) reports the deviation of the local particle density from the mean density. In the range of 23−

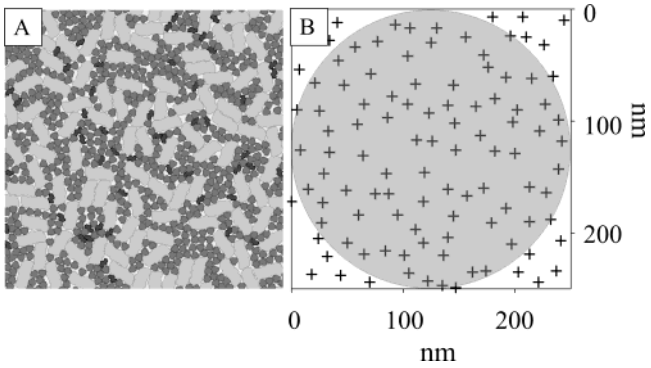

FIGURE 3: Determination of the PSII position in a purely random protein distribution. Panel A shows an example of a random distribution of $(PSII-LHCII_3)_2$ supercomplexes (light gray), $LHCII_3$ (gray), and cyt bf dimers (dark gray) calculated with the Monte Carlo simulation. The protein density is the same as that determined for the stacked grana regions (see text). Panel B shows the distribution of the centers of the PSII supercomplexes.

24 nm, the PSII density displays a distinct maximum, indicating a local density about 1.4 times greater than the mean.

Comparison of the PSII Distribution in Grana Membranes with a Random Distribution. For further investigations, random distributions of LHCII trimers, cyt bf dimers, and PSII supercomplexes were calculated with a Monte Carlo simulation to allow the comparison with the PSII distribution in grana membranes of chloroplasts. Published contours of LHCII trimers (*9*), cyt bf dimer (*56*), and $(PSII-LHCII_3)_2$ supercomplex (*14*) were used for these calculations. The particle density for LHCII and PSII supercomplexes was chosen according to the values determined for core grana membranes (see above). For the density of the cyt bf complex, a cyt bf to PSII ratio of 0.5 is assumed (*20*). This ratio should be taken as an upper limit because it was calculated from Table 1 for the whole thylakoid membrane and, while PSII is concentrated in the grana, cyt bf complexes are more homogeneously distributed. We also analyzed distributions without cyt bf complexes. No significant differences were seen compared with results including the cyt bf complex (not shown). This is to be expected, since the relative area occupation of the cyt bf complex in the granum is only a few percent. An example for the distribution of particles resulting from a Monte Carlo simulation, together with the coordinates of PSII supercomplexes deduced from it, is shown in Figure 3. For the calculations, we assumed no interactions between the complexes, except for hard-core repulsion. Therefore, these distributions represent a purely random protein organization.

The analysis of the PSII supercomplex distribution from the Monte Carlo simulation compared to the EF_s analysis is summarized in Figure 4. In the next neighbor analysis (Figure 4A), as well as in PCF (Figure 4B), significant differences are visible between the random Monte Carlo distribution and the EF_s distribution. In the EF_s particle distribution, distances between 11 and 15 nm and between 17 and 21 nm occurred less often (Figure 4A) than in the random distribution. This suggests that, looking from a typical PSII particle, photosystems in the immediate proximity and at a distance of about 20 nm are less abundant than in a random distribution. In contrast, in distances between 15 and 17 nm and between 21 and 25 nm the EF_s particles have a higher abundance.

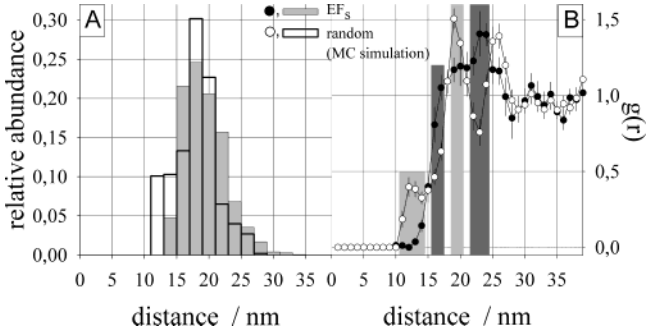

FIGURE 4: Comparison of the distribution of next neighbor distances (A) and PCF (B) analysis of EF_s particles with the random PSII distribution calculated by Monte Carlo simulation. A total of 1060 particles from 10 Monte Carlo distributions on areas of 250 nm × 250 nm and 1016 particles from 12 EF_s pictures were analyzed. The error bars in the PCF indicate the standard error of the mean. The light gray bars in panel B indicate distances of a decreased EF_s density compared to the random Monte Carlo distribution, whereas dark gray bars indicate an increased density.

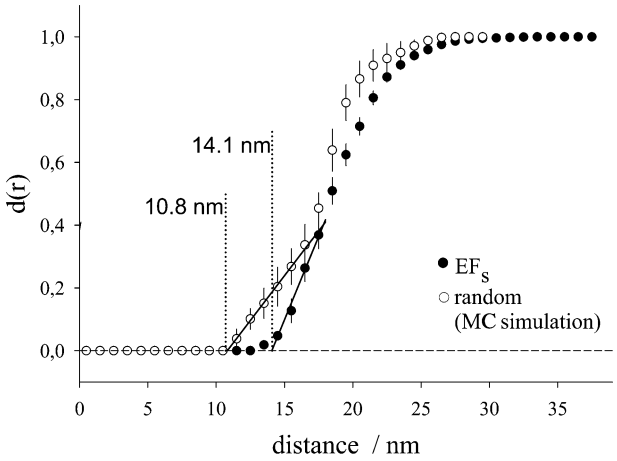

FIGURE 5: Comparison of the NNDF analysis, $d(r)$, of EF_s particles and Monte Carlo (MC) simulations. Data were calculated from Figures 2A and 4A. The intersections with the abscissa were deduced from a linear regression of values up to $d(r) = 0.4$. Note the displacement of the EF_s data for larger distances. The errors bars indicate the standard error of the mean.

These deviations in the next neighbor distribution correspond to changes in the local particle density analyzed by PCF (Figure 4B). Both analyses of the particle distribution give clear evidence that the organization of PSII in stacked grana areas is different from a random distribution.

Further information about the particle distribution in the EF_s half-membrane can be deduced from the NNDF (Figure 5), which was calculated from the data in Figures 2A and 4A. The mean nearest neighbor distance of the distance distribution of the purely random protein ensemble is 17.9 nm, and thereby shorter than is the case for the stacked grana membranes (19.4 nm). The nearest possible distance between two neighboring PSII supercomplexes can be deduced from the intersection of the NNDF data with the abscissa. This distance is about 11 nm for the Monte Carlo simulation and about 14 nm for the EF_s distribution (Figure 5).

Diffusion of PSII. To investigate PSII mobility in a membrane with a protein density typical for grana thylakoids, Monte Carlo distributions were generated. The complexes were then moved in a random direction on a square lattice with a step width of 1 nm corresponding to the size of a lipid headgroup. The step is allowed if the proposed position

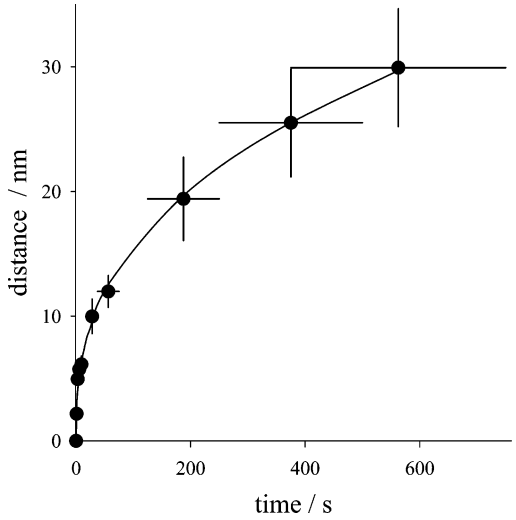

FIGURE 6: Mean diffusion distance of PSII as a function of time in Monte Carlo simulations. The horizontal error bars are given by the range of diffusion coefficients D (2×10^{-12} to 4×10^{-12} cm^{-2} s^{-1}). The time scale is calculated from the number of Monte Carlo steps (1 nm step width) with the Einstein equation $t = \langle x \rangle^2/4D$. One step corresponds to 0.625−1.250 ms. The displacement of a PSII complex (y-axis) was determined after 1000 (corresponding to 0.9375 ± 0.3125 s) to 600 000 (corresponding to 562.5 ± 187.5 s) Monte Carlo steps on a 35 nm × 35 nm matrix. Each point is the mean of at least 10 PSII analyzed. Vertical error bars indicate the standard deviation.

is not already occupied by another protein particle. Otherwise the particle remains in its original position. In this way, it is possible to simulate the diffusion in a membrane. A measure for the velocity of the PSII movement is gained from the mean distance reached by a PSII after a given number of Monte Carlo steps. A Monte Carlo step can be transformed into a physical time scale with the help of the two-dimensional Einstein equation ($\Delta x^2 = 4Dt$). For this calculation, a diffusion coefficient of PSII (D) must be assumed. Unfortunately the data available for estimating this are poor. For the trimeric LHCII, published values lie between 2×10^{-12} and 4×10^{-12} cm^2 s^{-1} (*57*). These diffusion coefficients are about 2 orders of magnitude smaller than those for protein complexes of similar sizes in the mitochondrial inner membrane (*58*). As discussed in ref *57*, this could be attributed to the interaction of the protein complexes in the grana thylakoids. Since it is to be expected that this interaction is also relevant for the movement of the $(PSII-LHCII_3)_2$ supercomplex, the values from ref *57* for the trimeric LHCII were used for the transformation of the number of Monte Carlo steps into a time scale for the PSII supercomplex (Figure 6). This assumption is supported by an indirect determination of the PSII diffusion coefficient (*59*). In this study, chlorophyll fluorescence changes of restacked thylakoids after unstacking was examined. A diffusion coefficient of $(1.8-10) \times 10^{-12}$ cm^2 s^{-1} for PSII was determined for temperatures between 10 and 24 °C. Because data about the diffusion coefficients of photosynthetic protein complexes are poor, our results must be taken as a first approximation for the description of PSII diffusion within grana membranes.

In the Monte Carlo simulation, the mean distance that a PSII supercomplex travels in 1 min is about 10 nm (Figure 6). This means that a complex moves only about half the size of its own dimension in a minute. In comparison, the Einstein equation predicts a 20−40 times higher mean displacement for a free particle. This enormous discrepancy is mainly a result of the high protein density (*60*). The Einstein equation is only valid for diluted particles. Because of the extremely high density of obstacles, the diffusion process of PSII supercomplexes in grana membranes is drastically impaired.

DISCUSSION

Nonrandom PSII Distribution in Grana Membranes. The analysis of the EF_s distribution in isolated chloroplasts gives two clear lines of evidence that the organization of photosystem II in this subcompartment is not random. (i) The comparison between the PCF analysis of grana membranes and a random distribution of protein complexes calculated by a Monte Carlo simulation shows a significant decrease in photosystem II concentration in a distance range between 11 and 15 nm and around 20 nm and an increased concentration around 17 nm and between 21 and 25 nm (Figure 4B). (ii) The pattern of next neighbor distances of PSII supercomplexes in grana membranes differs from a random protein organization (Figure 4A). The NNDF analysis (Figure 5) reveals that, compared to a purely random distribution, PSII complexes in the intact grana core membrane are further separated. These results confirm and quantify the intuitive impression that the EF particles in the grana area of thylakoid membranes "repel" each other (*61*).

Besides the clear evidence for order in PSII organization in grana thylakoids, there is also a randomizing influence visible. In the extreme case of a totally ordered protein organization, only one distance would occur in the distribution of the nearest neighbor distances and in the PCF maxima would occur at multiples of the lattice distance (*44*). In contrast, the distribution of next neighbor distances and the PCF analysis of the grana thylakoids show a distinctly different behavior (Figure 2). Thus, the PSII arrangement in grana membranes is between a purely random and a totally ordered distribution.

Similar results to intact chloroplasts were also obtained from isolated BBY grana membranes (Figure 7). It is noteworthy that BBY preparations contain no cyt bf complex. This implies that the supramolecular protein distribution in stacked grana thylakoids is mainly determined by LHCII and PSII and not by cyt bf complexes.

Our data indicate that, in addition to pure hard-core steric repulsion, there is an interaction force operating in grana thylakoids, which tends to separate the PSII supercomplexes (Figure 5). The molecular reasons for these interactions are unclear. It is possible that the lipid environment of the supercomplexes plays an important role (*62*). For example, the catalytic hydrogenation of highly unsaturated fatty acid in thylakoid lipids causes an alteration in LHCII−PSII interactions, which can be explained as a dissociation of LHCII trimers from the PSII complex (*63*). Furthermore, the detergent-induced pronounced formation of paracrystalline protein arrays in grana membranes of cold-stressed plants indicates the importance of the saturation level of lipid fatty acids for the protein interactions (*31*). However, further research is necessary to understand the protein interactions in thylakoid membranes. It is noteworthy that the contour of isolated protein complexes used for the Monte Carlo

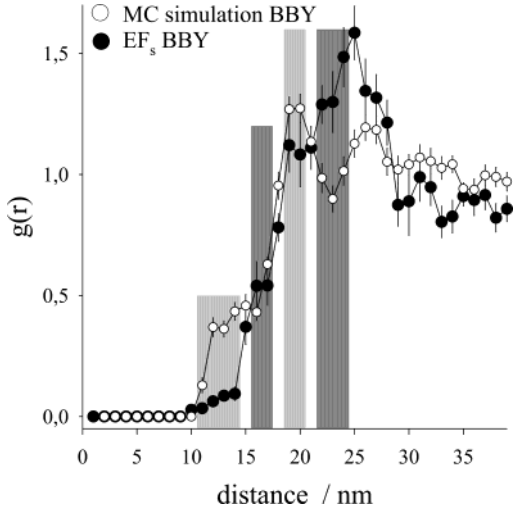

FIGURE 7: PCF analysis of the PSII distribution in isolated grana membranes (BBY). A total of 448 particles from seven electron micrographs were analyzed. The bars indicate density changes between the EF_s distributions and Monte Carlo distributions for intact chloroplasts taken from Figure 4B. The errors bars indicate the standard error of the mean.

simulation is corrected for their detergent shell. The natural lipids could explain the observed separation of photosystems II in the core granum (Figure 5). This will be discussed below.

Supramolecular Interpretation of the PSII Distribution. An important result of this work is that the nearest neighbor distance of two adjacent PSII supercomplexes in EF_s distributions is greater (14 nm) than in random Monte Carlo distributions (11 nm) (Figure 5). A minimal distance of 11 nm between two photosystems occurs due to a direct contact at the longer sides of the supercomplexes (Figure 8A). Corresponding pairs of photosystem are recognizable in the Monte Carlo picture (Figure 3A). A possible explanation for the increased distance in the EF_s half-membrane is that supercomplexes are surrounded by a shell of strongly attached boundary lipids (Figure 8B). The resulting separation of PSII would also lead to the increased abundance of distances between 15 and 17 nm and the decrease between 11 and 15 nm in the next neighbor analysis of the EF_s distributions (Figure 4A). In fact, there is evidence from biochemical studies and measurements with spin-labeled lipids that protein complexes in the thylakoid membrane are separated by boundary lipids (see ref *34*). This lipid-induced separation could be important for the accessibility of plastoquinones to the QB binding niche of photosystem II. The suspected positions for binding niches (*14*) are marked with gray arrows in Figure 8A,B.

The comparison of the analysis of EF_s with random distributions allows distances that are caused by interaction forces other than simple hard-core repulsion to be screened for. These distances should have an increased abundance in the next neighbor analysis (Figure 4A). In the NNDF, distances between 21 and 25 nm occur more often in the EF_s distribution than in the random distribution. It is possible to interpret this result on a supramolecular level based on the recently discovered LHCII binding sites at the PSII−LHCII supercomplex (*25*, *26*). Four discrete LHCII binding sites at the $(PSII-LHCII_3)_2$ supercomplex have been identified. Looking at the contour of the supercomplex as an

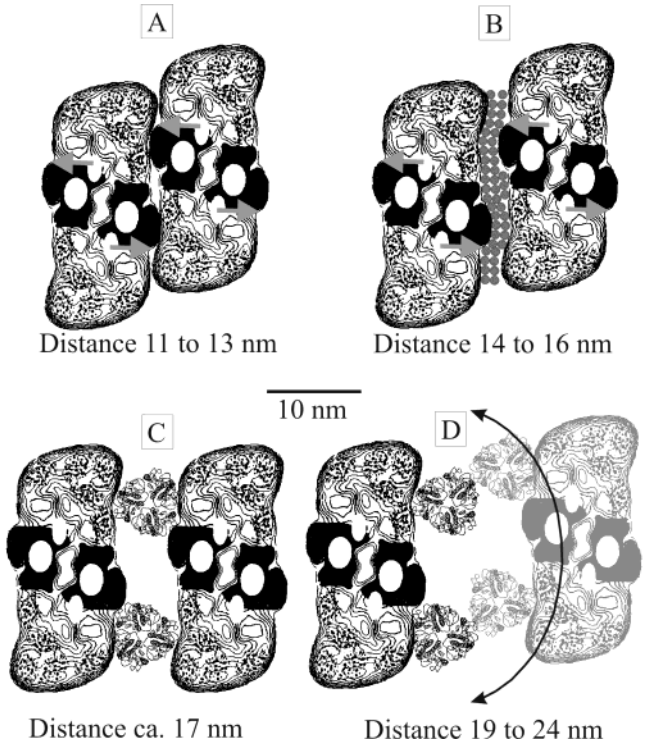

FIGURE 8: Tentative constructs of PSII supercomplexes and LHCII trimers. The structures of the complexes were taken from ref *14* for PSII and ref *9* for LHCII. The binding sites of LHCII trimers at the PSII−LHCII supercomplex are taken from refs *25* and *26*. Gray arrows in panels A and B indicate suggested QB binding sites at the PSII supercomplex. Gray circles in panel B represent lipids (1 nm diameter).

approximately 12 nm × 27 nm rectangle, all four binding sites are located on the longer sides of the rectangle, specifically at the top and bottom ends (*26*). Based on these data, two models were constructed in which PSII−LHCII supercomplexes are separated from each other by two (Figure 8C) or four (Figure 8D) LHCII trimers. In these models, the separation of two photosystems is minimal, since boundary lipids were not taken into account (direct protein contact). Two associations comparable to Figure 8C were recently described for grana membranes (*26*) and were called megacomplexes. The PSII−PSII distance of 20 nm in both megacomplexes is bigger than that in Figure 8C (17 nm). As discussed above, this could be explained by strongly bound boundary lipids. However, distances between 17 and 21 nm are less abundant in the EF_s distribution compared to the Monte Carlo distribution (Figure 4A). This indicates that in the grana there is no driving force toward the construction of megacomplexes such as those shown in Figure 8C.

The increased abundance of distances between 21 and 25 nm in the EFs half-membrane could be explained by a model shown in Figure 8D. This arrangement is based on the assumption that in the stacked grana area all binding sites for LHCII at the PSII supercomplex are occupied (*25*, *26*). By rotating the right LHCII−PSII construct (gray in Figure 8D) around the left construct (black in Figure 8D) different distances between 19 and 24 nm can be generated. Boundary lipids could lead to further separation. The suggested model in Figure 8D could explain the increased abundance of distance between 21 and 25 nm in the EF_s half-membrane (Figure 4A). Furthermore this arrangement is attractive since there would be space for a dimeric cyt bf complex between

the protein complexes. This was postulated in the so-called "microdomain" concept deduced from functional measurements (*33*, *61*). The accessibility of the plastoquinone binding niche at PSII and cyt bf complex could be optimized by "microdomains". At present, however, the model in Figure 8D should be understood as a suggestion that needs further verification.

It is noteworthy that PSII distances other than those discussed above occur in the grana core. However, these distances are not more abundant than expected from a purely random distribution.

Lateral PSII Diffusion. The diffusion analysis of the $(PSII-LHCII_3)_2$ supercomplex in the Monte Carlo simulation gives an impression of how restricted the mobility of this protein complex is in a randomly organized membrane with a protein density like that of grana thylakoids. In 1 min, the complex would only move about 10 nm, half of its own size. Extrapolating the data with a root function for prolonged times, it is possible to estimate the PSII supercomplex movement for longer times (Figure 6, line). The mobility of the PSII supercomplex is important for the lateral transport from grana thylakoids to the stroma lamellae during the repair cycle of photoinhibited PSII (*40*). The primary photodamage of PSII takes place in the grana membranes, whereas repair of the damaged PSII, including D1 degradation and the insertion of de-novo synthesized D1 takes place in stroma-exposed membranes. Thus, the accessibility of the enzymes of the repair cycle localized in the unstacked thylakoid membranes requires a lateral transport of PSII out of the grana membranes. In a grana disk with a diameter of 400−500 nm (*2*, *3*), the mean migration distance for half of the PSII into unstacked regions is 60−70 nm. By the extrapolation mentioned above, a half-time of about 1 h can be predicted for a movement of this distance. Notably, the half-time for D1 degradation falls into the same time range (*64*). This suggests that the diffusion rate of the PSII complexes out of the grana area could have a strong influence on the speed of the repair cycle of photoinhibited PSII. It is likely that the photoinhibited PSIIs do not diffuse as a complete supercomplex into stroma lamellae but that flanking Lhcb proteins are already removed (*37*). Probably this complex could diffuse at a higher speed, due to its smaller size. In this context, it is noteworthy that the diffusion coefficients reported for the trimeric LHCII (*57*) and PSII (*59*) have similar values, even though their size is clearly different. This indicates that the size of the protein complexes plays a minor role in the diffusion process in grana membranes. Unfortunately, the diffusion coefficients of protein complexes in the thylakoid membrane are not very well-known. Furthermore, little is known about the impact of protein−protein and protein−lipid interactions in diffusion processes in thylakoids. Nevertheless, our analysis indicates that the hindered PSII diffusion in the densely packed thylakoid membrane may have a decisive influence on migration processes between grana membranes and stroma lamellae.

Physiological Significance of the PSII Distribution in Grana Membranes. The protein density determined in grana thylakoids of about 80% is very high (see Figure 4A). This result confirms recent data quantifying the protein area in the thylakoid membrane based on a stoichiometric analysis of lipids and protein complexes (*34*, *35*). An obvious explanation for the high protein density could be that, together with the proteins, pigments bound to the light-harvesting complexes also have a high concentration in the thylakoid membrane. Therefore, it is highly probable that light passing through a chloroplast will be absorbed and available for use in photosynthesis. However, a high protein density may also cause problems. Plastoquinone diffusion in the thylakoid membrane might be hindered by the large number of diffusion obstacles (e.g., see refs *33*, *35*, *61*, *65*, and *66*). This is of great physiological relevance, since the PQ pool has an important sensor function for several regulatory processes (*37*−*39*) and a long-lasting reduction of PQ at the QB binding site leads to photoinhibition of PSII (*40*, *67*). This study gives evidence that the involvement of boundary lipids and specific interactions between light-harvesting complexes could have an organizing effect on the supramolecular arrangement of PSII supercomplexes and LHCII trimers. Lipids and LHCII trimers positioned between PSII complexes could keep these at a certain distance. Direct contact of PSII complexes at their longer sides is thus avoided. This would ensure the accessibility of the QB binding niche for plastoquinone, which is positioned on this side (*15*) and allow an efficient electron transfer from PSII to PQ.

Beside these structuring factors, there also exist randomizing forces in the supramolecular protein organization in grana thylakoids. In contrast to photosynthetic bacteria, in which a highly ordered but rigid organization of light-harvesting complexes and photosystems is realized (*68*), the arrangement in grana membranes is a mixture of random distributions and highly ordered arrangements. This can be explained by relatively low interaction energy between the protein complexes in grana. In this case, the protein arrangement is significantly influenced by Brownian movement and represents the result of this randomizing force and the structure-inducing interactions. The thylakoid membrane is a highly dynamic membrane, in which the permanent rearrangement of the protein organization is an adaptive response to changing environmental conditions (*2*, *38*). It is possible that the necessary flexibility of the protein organization is facilitated by the significant contribution of the Brownian molecular movement. This would be an evolutionary development, compared to the rigid protein arrangement in photosynthetic bacteria.

ACKNOWLEDGMENT

We thank Conny Vinnemann and Dr. Giles N. Johnson for help with the manuscript.

REFERENCES

1. Arvidsson, P.-O., and Sundby, C. (1999) A model for the topology of the chloroplast thylakoid membrane, *Aust. J. Plant Physiol. 26*, 687−694.
2. Staehelin, L. A., and van der Staay, G. W. M. (1996) Structure, composition, functional organization and dynamic properties of thylakoid membranes, in *Oxygenic photosynthesis: The light reactions* (Ort, D. A., and Yocum, C. F., Eds.) pp 11−30, Kluwer Academic Publishers, Dordrecht, Netherlands.
3. Albertsson, P.-A. (2001) A quantitative model of the domain structure of the photosynthetic membrane, *Trends Plant Sci. 6*, 349−354.
4. Kühlbrandt, W., Wang, D. N., and Fujiyoshi, Y. (1994) Atomic model of plant light-harvesting complex by electron crystallography, *Nature 367*, 614−621.

5. Rhee, K.-H., Morris, E. P., Barber, J., and Kühlbrandt, W. (1998) Three-dimensional structure of plant photosystem II reaction centre at 8 Å resolution, *Nature 396*, 283−286.
6. Kamiya, N., and Shen, J.-R. (2003) Crystal structure of oxygen-evolving photosystem II from *Thermosynechococcus vulcanus* at 3.7-Å resolution, *Proc. Natl. Acad. Sci. U.S.A. 100*, 98−103.
7. Jordan, P., Fromme, P., Witt, H. T., Klukas, O., Saenger, W., and Krauss, N. (2001) Three-dimensional structure of cyanobacterial photosystem I at 2.5 Å resolution, *Nature 411*, 909−917.
8. Groth, G., and Pohl, E. (2001) The structure of the chloroplast F1 ATPase at 3.2 Å resolution, *J. Biol. Chem. 276*, 1345−1352.
9. Kühlbrandt, W., and Wang, D. N. (1991) Three-dimensional structure of plant light-harvesting complex determined by electron crystallography, *Nature 350*, 130−134.
10. Jansson, S. (1994) The light-harvesting chlorophyll a/b binding proteins, *Biochim. Biophys. Acta 1184*, 1−19.
11. Hope, A. B. (1993) The chloroplast cytochrome bf complex: a critical focus on function, *Biochim. Biophys. Acta 1143*, 1−22.
12. Bron, P., Lacapère, J.-J., Breyton, C., and Mosser, G. (1999) The 9 Å projection structure of cytochrome b_6f complex determined by electron crystallography, *J. Mol. Biol. 287*, 117−126.
13. Ben-Shem A., Frolow, F., and Nelson, N. (2003) Crystal structure of plant photosystem I, *Nature* 426, 630−635.
14. Hankamer, B., Barber, J., and Boekema, E. J. (1997) Structure and membrane organization of photosystem II in green plants, *Annu. Rev. Plant Physiol. Plant Mol. Biol. 48*, 641−671.
15. Nield, J., Orlova, E. V., Morris, E. P., Gowen, B., van Heel, M., and Barber, J. (2000) 3D map of the plant photosystem II supercomplex obtained by cryoelectron microscopy and single particle analysis, *Nat. Struct. Biol. 7*, 44−47.
16. Hankamer, B., Nield, J., Zheleva, D., Boekema, E., Jansson, S., and Barber, J. (1997) Isolation and biochemical characterisation of monomeric and dimeric photosystem II complexes from spinach and their relevance to the organisation of photosystem II in vivo, *Eur. J. Biochem. 243*, 422−429.
17. Morissey, P. J., Glick, R. R., and Melis, A. (1989) Supramolecular assembly and function of subunits associated with the chlorophyll a−b light-harvesting complex II (LHC II) in soybean chloroplasts, *Plant Cell Physiol. 30*, 335−344.
18. Stoylova, S., Flint, T. D., Ford, R. C., and Holzenburg, A. (2000) Structural anaylsis of photosystem II in far-red-light-adapted thylakoid membranes. New crystal forms provide evidence for a dynamic reorganization of light-harvesting antennae subunits, *Eur. J. Biochem. 267*, 207−215.
19. Bumba, L., and Vácha, F. (2003) Electron microscopy in structural studies of photosystem II, *Photosynth. Res. 77*, 1−19.
20. Yu, S.-G., Björn, G., and Albertsson, P.-A. (1993) Characterization of a non-detergent PSII − cytochrome b/f preparation (BS), *Photosynth. Res. 37*, 227−236.
21. Santini, C., Tidu, V., Tognon, G., Magaldi, A. G., and Bassi, R. (1994) Three-dimensional structure of the higher plant photosystem II reaction centre and evidence for its dimeric organization in vivo, *Eur. J. Biochem. 221*, 307−315.
22. Boekema, E. J., Hankamer, B., Bald, D., Kruip, J., Nield, J., Boonstra, A. F., Barber, J., and Rögner, M. (1995) Supramolecular structure of the photosystem II complex from green plants and cyanobacteria, *Proc. Natl. Acad. Sci. U.S.A. 92*, 175−179.
23. Nield, J., Kruse, O., Ruprecht, J., Fonseca, P. da, Büchel, C., and Barber, J. (2000) Three-dimensional structure of chlamydomonas reinhardtii and synechococcus elongatus photosystem II complexes, *J. Biol. Chem. 275*, 27940−27946.
24. Yakushevska, A. E., Jensen, P. E., Keegstra, W., van Roon, H., Scheller, H. V., Boekema, E. J., and Dekker, J. P. (2001) Supermolecular organization of photosystem II and its associated light-harvesting antenna in *Arabidopsis thaliana*, *Eur. J. Biochem. 268*, 6020−6028.
25. Harrer, R. (2003) Associations between light-harvesting complexes and photosystem II from *Marchantia polymorpha* L. determined by two- and three-dimensional electron microscopy, *Photosynth. Res. 75*, 249−258.
26. Boekema, E. J., van Roon, H., Calkoen, F., Bassi, R., and Dekker, J. P. (1999) Multiple types of association of photosystem II and its light-harvesting antenna in partially solubilized photosystem II membranes, *Biochemistry 38*, 2233−2239.
27. Simpson, D. J. (1978) Freeze-fracture studies on barley plastid membranes II. Wild-type chloroplasts, *Carlsberg Res. Commun. 43*, 365−389.
28. Lyon, M. K., and Miller, K. R. (1985) Crystallization of the light-harvesting chlorophyll complex within thylakoid membranes, *J. Cell Biol. 100*, 1139−1147.
29. Seibert, M., DeWit, M., and Staehelin, L. A. (1987) Structural localization of the O_2-evolving apparatus to multimeric (tetrameric) particles on the lumenal surface of freeze-etched photosynthetic membranes, *J. Cell Biol. 105*, 2257−2265.
30. Vallon, O., Tae, G. S., Cramer, W. A., Simpson, D., Hoyer-Hansen, G., and Bogorad, L. (1989) Visualization of antibody binding to the photosynthetic membrane: the transmembrane orientation of cytochrome b-559, *Biochim. Biophys. Acta 975*, 132−141.
31. Lyon, M. K. (1998) Multiple crystal types reveal photosystem II to be a dimer, *Biochim. Biophys. Acta 1364*, 403−419.
32. Boekema, E. J., van Breemen, J. F. L., van Roon, H., and Dekker, J. P. (2000) Arrangement of photosystem II supercomplexes in crystalline macrodomains within the thylakoid membrane of green plant chloroplast, *J. Mol. Biol. 301*, 1123−1133.
33. Kirchhoff, H., Horstmann, S., and Weis, E. (2000) Control of the photosynthetic electron transport by PQ diffusion microdomains in thylakoids of higher plants, *Biochim. Biophys. Acta 1459*, 148−168.
34. Kirchhoff, H., Mukherjee, U., and Galla, H.-J. (2002) Molecular architecture of the thylakoid membrane: Lipid diffusion space for plastoquinone, *Biochemistry 41*, 4872−4882.
35. Tremmel, I. G., Kirchhoff, H., Weis, E., and Farquhar, G. D. (2003) Dependence of plastoquinone diffusion on the shape, size, and density of integral thylakoid proteins, *Biochim. Biophys. Acta 1607*, 97−109.
36. Rintamäki, E., and Aro, E.-M. (2001) Phosphorylation of photosystem II proteins, in *Regulation in photosynthesis* (Aro, E.-M., and Andersson, B., Eds.) pp 395−418, Kluwer Academic Publishers, Dordrecht, The Netherlands.
37. Kruse, O. (2001) Light-induced short-term adaptation mechanisms under redox control in the PSII-LHCII supercomplexes: LHCII state transition and PSII repair cycle, *Naturwissenschaften 88*, 284−292.
38. Allen, J. F. (2003) State transitions − a question of balance, *Science 299*, 1530−1532.
39. Pfannschmidt, T., Allen, J. F., and Oelmüller, R. (2001) Principles of redox control in photosynthesis gene expression, *Physiol. Plant. 112*, 1−9.
40. Andersson, B., and Aro, E.-M. (2001) Photodamage and D1 protein turnover in photosystem II, in *Regulation in photosynthesis* (Aro, E.-M., and Andersson, B., Eds.) pp 377−393, Kluwer Academic Publishers, Dordrecht The Netherlands.
41. Bernhardt, K., and Trissl, W. (1999) Theories for kinetics and yields of fluorescence and photochemistry: how, if at all, can different models of antenna organization be distinguished experimentally? *Biochim. Biophys. Acta 1409*, 125−142.
42. Nairn, J. A., Haehnel, W., Reisberg, P., and Sauer, K. (1982) Picosecond fluorescence kinetics in spinach chloroplasts at room temperature. Effects of Mg^{2+}, *Biochim. Biophys. Acta 682*, 420−429.
43. Pearson, L. T., Edelman, J, and Chan, S. I. (1984) Statistical mechanics of lipid membranes. Protein correlation functions and lipid ordering, *Biophys. J. 45*, 863−871.
44. Kubitscheck, U., and Peters, R. (1998) Localization of single nuclear pore complexes by confocal scanning microscopy and analysis of their distribution, *Methods Cell Biol. 53*, 79−98.
45. Kubitscheck, U., Kues, T., and Peters, R. (1999) Visualization of nuclear pore complex and its distribution by confocal laser scanning microscopy, *Methods Enzymol. 307*, 207−230.
46. Randall, P. J., and Bouma, D. (1973) Zinc deficiency, carbonic anhydrase, and photosynthesis in leaves of spinach, *Plant Physiol. 52*, 229−232.
47. Berthold, D. A., Babcock, G. T., and Yocum, C. F. (1981) A highly resolved, oxygen-evolving photosystem II preparation from spinach thylakoid membranes, *Fed. Eur. Biochem. Soc. 134*, 231−234.
48. Porra, R. J., Thompson, W. A., and Kriedermann, P. E. (1989) Determination of accurate extinction coefficient and simultaneous equations for essaying chlorophylls a and b extracted with four different solvents: verification of the concentration of chlorophyll standards by atomic absorption spectroscopy, *Biochim. Biophys. Acta 975*, 384−394.
49. L'Ecuyer, P. (1988) Efficient and portable combined random number generators. *Commun. Assoc. Comput. Mach. 31*, 742−774.

50. Press, W. H., Flannery, B. P., Teukolsky, S. A., and Vetterling, W. T. (1992) Numerical Recipes in C, in *The Art of Scientific Computing*, Chapter 7.1, 2nd edition, pp 275−286, Cambridge University Press, New York.
51. König, D., Carvajal-Gonzalez, S., Downs, A. M., Vassy, J., and Rigaut, J. P. (1990) Modelling and analysis of 3-D arrangements of particles by point processes with examples of application to biological data obtained by confocal scanning light microscopy, *J. Microsc. 161*, 405−433.
52. Diggle, P. J. (1983) *Statistical Analysis of Spatial Point Patterns*, Academic Press, London.
53. Karlsson, L. M., and Liljeborg, A. (1994) Second-order stereology for pores in translucent alumina studied by confocal scanning laser microscopy, *J. Microsc. 175*, 186−194.
54. McQuarrie, D. A. (1976) *Statistical Mechanics*, Harper Collins Publishers Inc., New York.
55. Peter, G. F., and Thornber, J. P. (1991) Biochemical composition and organization of higher plant photosystem II light-harvesting pigment−proteins, *J. Biol. Chem. 266*, 16745−16754.
56. Breyton, C. (2000) Conformational changes in the cytochrome b6f complex induced by inhibitor binding. *J. Biol. Chem. 275*, 13195−13201.
57. Drepper, F., Carlberg, I., Andersson, B., and Haehnel, W. (1993) Lateral diffusion of an integral membrane protein: Monte Carlo analysis of the migration of phsphorylated light harvesting-complex II in the thylakoid membrane, *Biochemistry 32*, 11915−11922.
58. Gupte, S., Wu, E.-S., Hoechli, L., Hoechli, M., Jacobson, K., Sowers, A. E., and Hackenbrock, C. R. (1984) Relationship between lateral diffusion, collision frequency, and electron transfer of mitochondrial inner membrane oxidation−reduction components, *Proc. Natl. Acad. Sci. U.S.A. 81*, 2606−2610.
59. Rubin, B. T., Barber, J., Paillotin, G., Chow, W. S., and Yamamoto, Y. (1981) A diffusional analysis of the temperature sensitivity of the Mg^{2+}-induced rise of chlorophyll fluorescence from pea thylakoid membranes, *Biochim. Biophys. Acta 638*, 69−74.
60. Saxton, M. J. (1994) Anomalous diffusion due to obstacles: a Monte Carlo study, *Biophys. J. 64*, 394−401.
61. Lavergne, J., Bouchaud, J.-P., and Joliot, P. (1992) Plastochinone compartimentation in chloroplasts. II. Theoretical aspects, *Biochim. Biophys. Acta 1101*, 13−22.
62. Siegenthaler, P. A., and Trémolières A. (1998) Role of acyl lipids in the function of photosynthetic membranes in higher plants, in *Lipids in photosynthesis: Structure, function and genetics* (Siegenthaler P.-A.; Murata N. Eds.) Chapter 8, pp 145−173, Kluwer Academic Publishers, Dordrecht, The Netherlands.
63. Horváth, G., Melis, A., Hideg, E., Droppa, M., and Vigh, L. (1987) Role of lipids in the organization and function of photosystem II studied by homogeneous catalytic hydrogenation of thylakoid membranes in situ, *Biochim. Biophys. Acta 891*, 68−74.
64. Rintamäki, E., Salo, R., Lehtonen, E., and Aro, E.-M. (1995) Regulation of D1-protein degradation during photoinhibition of photosystem II in vivo: Phosphorlyation of the D1 protein in various plant groups, *Planta 195*, 379−386.
65. Haehnel, W. (1984) Photosynthetic electron transport in higher plants, *Annu. Rev. Plant Physiol. 35*, 659−693.
66. Blackwell, M., Gibas, C., Gygax, S., Roman, D., and Wagner, B. (1994) The plastoquinone diffusion coeffizient in chloroplasts and its mechanistic implications, *Biochim. Biophys. Acta 1183*, 533−543.
67. Barber, J., and Andersson, B. (1992) Too much of a good thing: light can be bad for photosynthesis, *Trends Biochem. Sci. 17*, 61−66.
68. Walz, T., Jamieson, S. J., Bowers, C. M., Bullough, P. A., and Hunter, C. N. (1998) Projection structures of three photosynthetic complexes from *Rhodobacter sphaeroides*: LH2 at 6 Å, LH1 and RC-LH1 at 25 Å, *J. Mol. Biol. 282*, 833−845.

BI0494626